

**Viability of sub-0.4-nm diameter carbon nanotubes**N. Sano,<sup>1,\*</sup> M. Chhowalla,<sup>1,†</sup> D. Roy,<sup>2</sup> and G. A. J. Amaratunga<sup>1</sup><sup>1</sup>University of Cambridge, Department of Engineering, Trumpington St., Cambridge CB2 1PZ, United Kingdom<sup>2</sup>University of Cambridge, Department of Material Science, Pembroke St., Cambridge CB2 3QZ, United Kingdom

(Received 1 July 2002; published 12 September 2002)

Hartree-Fock (HF) and density functional theory calculations indicate that a (4,0) carbon nanotube (CNT) of sub-0.4-nm diameter is stable and its heat of formation is close to that of the stable  $C_{36}$  ( $D_{6h}$ ). Semiempirical molecular-orbital calculation shows that such narrow tubular structure is more stable than the corresponding opened fragment in the innermost zone of a large CNT. Simulated TEM images show that an extra-narrow CNT does not show the typical CNT image regardless of the microscopic resolution. In order to aid experimental identification, the Raman spectrum of the (4,0) CNT obtained from HF calculation shows  $A_{1g}$  breathing modes in  $489\text{--}725\text{ cm}^{-1}$ .

DOI: 10.1103/PhysRevB.66.113403

PACS number(s): 61.46.+w, 78.67.-n, 81.07.De

Over a decade of experimental and theoretical studies on carbon nanotubes (CNT's),<sup>1</sup> a commonly accepted view has been that 0.4 nm is the minimum limit for the CNT diameter. This is rooted in the theoretical estimation based on the size limit of the cap at the end of the CNT,<sup>2,3</sup> and on the energetic considerations.<sup>4</sup> For cap size limitation,  $C_{20}$  fullene molecule of 0.4-nm diameter is considered as the smallest. For energetic considerations, Sawada *et al.*<sup>4</sup> calculated the energy of a graphite ribbon with a width that was the same as the circumference of a CNT and compared it with the energy of a corresponding CNT. In their result, the total energy of the tubular structure was lower than the open ribbon structure when the tube diameter was above 0.4 nm. Their conclusion of 0.4 nm being the minimum diameter limit of a CNT may be valid provided that growth takes place in free space.

Here, we consider the growth conditions that may break this theoretical limit for the minimum diameter tube. We argue the case that carbon can be provided into the innermost zone inside a relatively large CNT. One example of such a process is the aligned growth of multiwalled (MW) CNT's by plasma enhanced chemical vapor deposition on a substrate.<sup>5</sup> In this growth process, carbon is decomposed from organic gases such as  $C_2H_2$  which diffuse through catalytic metal particles to start CNT growth. The important point in this growth mechanism is that C can be provided into the innermost zone inside MW CNT's through the catalytic particle. There are two main differences between CNT growth in free space and in a restricted zone like the innermost zone of a MW CNT: (i) The narrow tube formed in a large CNT can be open ended because this unstable end can be protected by the outer CNT shell from a highly reactive environment during the growth process so that the CNT diameter limit posed from the cap size does not apply. (ii) The volume in the innermost zone of the MW CNT is tightly restricted so that a metastable structure can be constrained by the inner walls of the MW CNT.

Here we consider an open ended (4,0) CNT as a possible candidate for the sub-0.4-nm CNT formed in the center of a MW CNT. The number of the carbon atoms was restricted to 64 because of the difficulty in obtaining a self-consistent field convergence for larger cluster sizes. The optimized

structure and its energy was calculated by Hartree-Fock (HF) and density functional theory (DFT's) methods using *S-VWN* (Refs. 6 and 7) and *B3-LYP* (Refs. 8 and 9) functionals with 3-21G basis set. The GAUSSIAN 98 package<sup>10</sup> was used to carry out these molecular-orbital (MO) calculations. Full structural optimization resulted in its average diameter and the length to be 0.33 and 1.54 nm.

The heat of formation of the ground-state (4,0) CNT from free C ( $^3P_0$ ) atoms along with experimentally observed fullerenes [ $C_{60}$ ,  $C_{36}$  ( $D_{6h}$ ),  $C_{20}$ ] and infinite two-dimensional (2D) graphite using three methods is shown in Table I. One can see the same trend in these HF and DFT's results. Among them, the *B3LYP/3-21G* gives the best agreement of well-known carbon structures reported by others.<sup>4,11-15</sup> The most stable structure in Table I is the infinite graphite sheet, as expected, followed by the  $C_{60}$  molecule,  $C_{36}$ , H-terminated (4,0), open ended (4,0) CNT, and  $C_{20}$ . The energy values obtained for a 64-atom (4,0) 3.3-Å CNT using the DFT (*B3LYP/3-21G*) method is  $-6.03\text{ eV/atom}$ , decreasing to  $-6.40\text{ eV/atom}$  when its end effect is minimized by hydrogen termination. This result suggests that a (4,0) CNT can also be stable enough to be synthesized under appropriate conditions because the structures of comparable stability such as the  $C_{20}$  and the  $C_{36}$  have been indeed synthesized in an ambient environment.<sup>16,17</sup> Other recent work by Peng *et al.*<sup>18</sup> who calculated the mechanical stability of some sub-0.4-nm CNT's using tight-binding molecular simulations also suggests that (4,0) is a stable structure.

We have employed a method similar to that of Sawada *et al.*<sup>4</sup> They compared the total energy of CNT with that of an open graphite ribbon with a width equivalent to the circumference of the CNT. Here, we use a semiempirical MO calculation using the AM1 Hamiltonian<sup>19</sup> on an H-terminated short cluster. We have used H-terminated (4,0) CNT with 32 C atoms and the uncurling ribbon obtained from the splitting of the CNT. In our work, we compare the energy of the CNT and the ribbon inside a larger (12,0) CNT. The top view of the (4,0) CNT placed inside (12,0) CNT is shown in Fig. 1(a). The projected bond angle  $\Phi$  determines the degree of uncurling of the (4,0) CNT. As  $\Phi$  is increased from  $135^\circ$  to  $180^\circ$ , the inner structure opens from a (4,0) CNT to a flat

TABLE I. Heat of formation from C atoms to clusters.

Calculated structure	Number of C atoms	Heat of formation (eV/atom)			Reference
		HF /3-21G	S-VWN /3-21G (DFT)	B3LYP /3-21G (DFT)	
$C_{60}$ ( $I_h$ )	60	-4.62	-8.521	-6.78	-6.89 <sup>a</sup> -6.96 <sup>b,c</sup> -6.94 <sup>d,e</sup>
$C_{20}$ ( $I_h$ )	20	-3.61	-7.71	-5.96	-5.85 <sup>e,f</sup>
$C_{36}$ ( $D_{6h}$ )	36	-4.19	-8.22	-6.45	-6.42 <sup>e,f</sup> -6.55 <sup>a</sup>
Open ended (4,0) CNT	64	-3.72	-7.81	-6.03	
H terminated (4,0) CNT <sup>g</sup>	64	-4.10	-8.21	-6.40	
Infinite 2D graphite <sup>h</sup>		-5.21	-9.05	-7.31	-7.52 <sup>a</sup> -7.40 <sup>i</sup> -7.23 <sup>j</sup>

<sup>a</sup>DFT [B3LYP/6-31(d)] by Ito *et al.* 2000 (Ref. 11).

<sup>b</sup>Experimental by Cioslowski, 1993 (Ref. 12).

<sup>c</sup>They reported the heat of formation from carbon atoms in 2D graphene to  $C_{60}$ . To obtain the value from free C atom, the heat of formation from free C to 2D graphene, -7.40 eV, is used for correction.

<sup>d</sup>Experimental by Steele *et al.*, 1992 (Ref. 13).

<sup>e</sup>HF by Feyereisen *et al.*, 1991 (Ref. 14).

<sup>f</sup>They reported the relative values among  $C_n$  ( $18 < n < 60$ ). Here, the heat of formation of  $C_{60}$ , -6.94 eV, was used for correction.

<sup>g</sup>Structural optimization was done by HF level. To obtain the energy of  $C_{64}$ , the energy of H atoms derived by an isodemic reaction scheme [ $6 \times (\text{H atom}) + C_6H_6 = 3C_2H_4$ ] is subtracted from the heat of formation of  $C_{64}H_8$ .

<sup>h</sup>Isodemic reaction scheme (Ref. 16) is used.

<sup>i</sup>Experimental by Sawada *et al.* (Ref. 4).

<sup>j</sup>Tight-binding by Ze-Xian, 2001 (Ref. 15).

ribbon. The position of the curled ribbon was energetically optimized at each  $\Phi$ . The heat of formation versus the uncurling angle  $\Phi$  for a (4,0) CNT in free space is shown in Fig. 1(b). Here, when the tube is only slightly open with a small  $\Phi$  ( $135\text{--}140^\circ$ ), there is a large increase in the energy of the structure due to the creation of dangling bonds at the opened edges. As the uncurling angle is increased beyond  $140^\circ$ ,  $\Delta E_f$  decreases due to the reduction in the stress induced by curvature. In free space,  $\Delta E_f$  is lower for  $\Phi = 180^\circ$  than for  $\Phi = 135^\circ$  indicating that the tubular structure is energetically less preferable than the graphene ribbon in this small size, consistent with the reports by Sawada *et al.*<sup>4</sup> However, the dependency of the energy versus the uncurling angle in a larger CNT is dramatically different as shown in Fig. 1(c). It can be seen that the energy sharply increases up to  $140^\circ$  similar to Fig. 2(b) and saturates between  $140^\circ$  and  $150^\circ$ . Above  $150^\circ$  the energy continues to increase sharply with  $\Phi$  due to the repulsion from the inner wall of the larger tube. If the outer nanotube has a larger diameter then the plateau region will simply shift to higher  $\Phi$ . The drastic en-

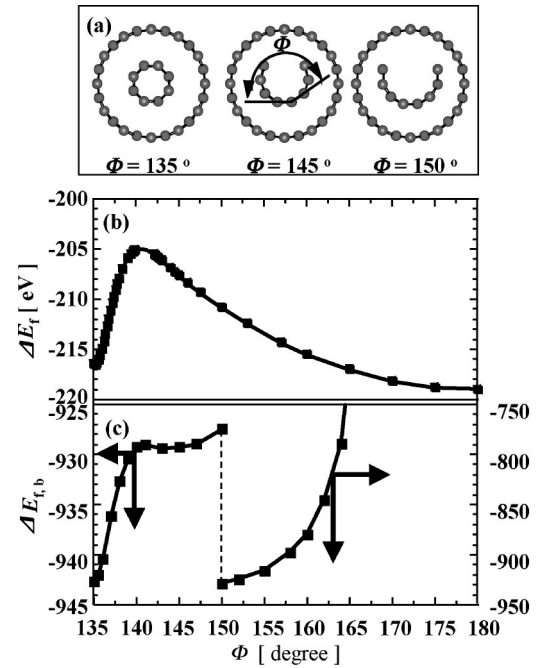


FIG. 1. Heat of formation from free atoms to the curled ribbon split from H-terminated (4,0) CNT,  $C_{32}H_8$ , (a) cross sectional image of curled ribbon in (12,0) CNT, (b)  $\Delta E_f$  in free space, and (c)  $\Delta E_{f,b}$  in (12,0) CNT.

ergy elevation at large  $\Phi$  indicates that the 0.4-nm minimum diameter theoretical limit suggested by Sawada *et al.*<sup>4</sup> is not applicable in the tightly restricted reaction zone within a MW CNT.

If indeed a (4,0) nanotube is feasible and can be fabricated then it must be observed using available analytical techniques. A highly useful technique for characterization of nanomaterials is high-resolution transmission electron mi-

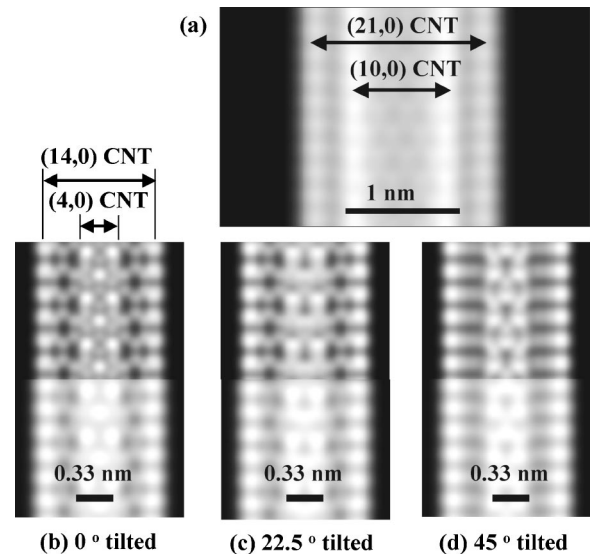


FIG. 2. Calculated atomic projection for double walled CNT's with (10,0) in (21,0), and (4,0) in (14,0): upper and lower in (b), (c), (d) are respectively for images in extra-high (atomically) and moderately high resolutions.

croscopy (HREM). In order to investigate the feasibility of utilizing HREM for locating a (4,0) CNT, we have calculated the projection of atoms from a double walled CNT with a (4,0) CNT as its inner core. The calculated projection gives a good indication of the expected atomically resolved HREM image of such a double walled CNT. In the calculation, the bright contrast of the projected atoms is determined by Gaussian distributions with their maximum at the atomic center. Here, all atoms are projected to produce the image and overlapping contrasts are enhanced through summation of each atomic contrast. Furthermore, the width of the Gaussian distribution of each atomic contrast was adjusted to simulate a very or moderately high atomic resolution. The calculated atomic projections of a typical MW CNT with a (10,0) nanotube within a larger (21,0) nanotube are shown in Fig. 2(a) to demonstrate the validity of the method. The very bright contrast at the location of the walls of the inner (10,0) CNT and the outer (21,0) CNT are readily visible. The result is in keeping with experiment in that the two pairs of lines representing the double walled CNT can be observed. The calculated atomic projections for a double walled CNT consisting of a (4,0) CNT within a larger (14,0) CNT are shown in Figs. 2(b)–(d). Projections in Figs. 2(b)–(d) were calculated at three tilting angles ( $0^\circ$ ,  $22.5^\circ$ ,  $45^\circ$ ) and at two resolutions. The significance of Figs. 2(b)–(d) is that the bright contrast for the (4,0) CNT is no longer a pair of parallel atomic lines typical of single walled CNT image but a unique pattern because of its significant tubular curvature. If the resolution is even lower, then the pattern becomes less clear, and it appear as a single thick line due to contrast overlapping. Therefore we believe that HREM is not a viable technique for observing a (4,0) CNT from our projection study. However, a report by Peng *et al.* claims the observation of 0.33 nm (4,0) CNT, a short tubular branch protruding from a 1.5-nm single walled CNT during electron beam irradiation in the HREM.<sup>18</sup> However, the branch showed tube walls as distinct parallel lines, inconsistent with our results. Close examination of their scale bar in the relevant figure reveals that the distance between the tube walls seems in fact 0.5 nm.

A more appropriate method, we believe, for verifying the existence of the (4,0) nanotube is Raman spectroscopy. The presence of the radial breathing modes of Raman spectrum have been correlated to of single walled CNT's by Saito *et al.*<sup>20</sup> If Saito's relationship is valid for sub-4-Å nanotubes, then a (4,0) nanotube with a diameter of 0.33 nm should give rise to a radial breathing mode at  $690\text{ cm}^{-1}$ . In order to investigate whether the (4,0) CNT can be observed in Raman, we have calculated its phonon modes using the HF (3-21 basis set) method. The calculated Raman spectrum obtained by HF/3-21G was corrected using a scaling factor of 0.9085 (Ref. 21) for electron correlation. We have tested the validity of our method by calculating the Raman modes of a  $C_{60}$  molecule and correlating them to theoretically and experimentally observed peaks. Our method shows good agreement with reported data of  $C_{60}$ .<sup>22–24</sup> The predicted Raman spectrum of the (4,0) CNT is shown in Fig. 3. The *G* and *D* peaks are prominently observed at  $1500\text{--}1600$  and  $1300\text{--}1420\text{ cm}^{-1}$ . In addition to these peaks, several modes in the

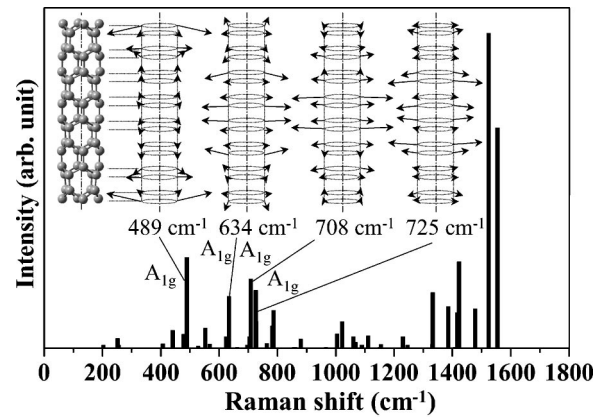


FIG. 3. Raman spectra on (4,0) CNT cluster,  $C_{64}$ , estimated by Hartree-Fock calculation (HF/3-21G): A scale factor, 0.9085, is used to correct the overestimation of the wave number caused by neglecting electron correlation. The relative atomic displacements in modes at  $489$ ,  $634$ ,  $708$ ,  $725\text{ cm}^{-1}$  are shown by arrows.

intermediate wave numbers ( $489\text{--}725\text{ cm}^{-1}$ ) can also be seen. These intermediate wave-number peaks are considered to be from the tube diameter  $A_{1g}$  breathing mode. In this figure, the atomic displacements for the significant peaks at  $489$ ,  $634$ ,  $708$ ,  $725\text{ cm}^{-1}$  are schematically shown using arrows.

Two DFT's using *S-VWN* and *B-LYP* (Ref. 25) functionals with 3-21G basis set were used to estimate the electronic energy levels of the 64-atom (4,0) CNT cluster model. To evaluate the validity of the method, the electronic energy levels of  $C_{60}$  were also calculated. The HOMO-LUMO gap obtained for the  $C_{60}$  fullerene by *S-VWN* and *B-LYP* levels were 1.83 and 1.82 eV, respectively. These values are higher only by 0.13 and 0.12 eV than the experimental value of 1.7 eV,<sup>26</sup> indicating reasonable agreement. Figure 4 shows the energy levels of the (4,0) CNT obtained by the *S-VWN* level, which is similar to that by *B-LYP*. The HOMO-lowest unoccupied (LUMO) gap obtained by both *S-VWN* and *B-LYP* was 0.08 eV. This is consistent with calculations which show

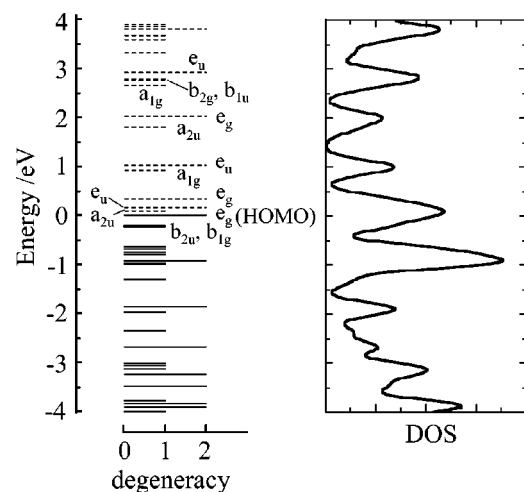


FIG. 4. Energy-level diagram and density of states (DOS) of the (4,0) CNT cluster,  $C_{64}$ , calculated by DFT (*S-VWN*/3-21G).

that a CNT predicted to be semiconducting by its chirality should become metallic if the diameter is significantly narrow because of the strong rehybridization of  $\sigma^*$  and  $\pi^*$  orbitals.<sup>27,28</sup> When the Raman shift is analyzed on such short (4,0) CNT's, we expect Raman resonance effects from the optically stimulated electronic transitions to discrete unoccupied energy levels.

In summary, energetic calculations by DFT show that the (4,0) CNT can be viable as its structural energy is very close to that of the C<sub>36</sub> (D<sub>6h</sub>) fullerene. Semiempirical MO calcu-

lations showed that the tubular structure is more stable than an open fragment in the innermost zone of a larger CNT, suggesting that extra-narrow CNT may be stable in such restricted zones. However, the atomic projection of (4,0) CNT indicates that such extra-narrow CNT will be difficult to observe using HREM regardless of the microscope resolution. As an alternative way to identify such a small (4,0) CNT, the Raman spectrum was predicted by HF calculation, showing significant A<sub>1g</sub> breathing modes in the wave-number range, 489–725 cm<sup>-1</sup>.

\*Permanent address: Himeji Institute of Technology, Department of Chemical Engineering, 2167, Shosha, Himeji, 671-2201, Japan.

†E-mail address: mc209@eng.cam.ac.uk

<sup>1</sup>S. Iijima, *Nature* (London) **354**, 56 (1991).

<sup>2</sup>L. Qin, X. Zhao, K. Hirahara, Y. Miyamoto, Y. Ando, and S. Iijima, *Nature* (London) **408**, 50 (2000).

<sup>3</sup>N. Wang, Z. K. Tang, G. D. Li, and J. S. Chen, *Nature* (London) **408**, 50 (2000).

<sup>4</sup>S. Sawada and N. Hamada, *Solid State Commun.* **83**, 917 (1992).

<sup>5</sup>M. Chhowalla, K. B. K. Teo, C. Ducati, N. L. Rupesinghe, G. A. J. Amaratunga, A. C. Ferrari, D. Roy, J. Robertson, and W. I. Milne, *J. Appl. Phys.* **90**, 5308 (2001).

<sup>6</sup>P. Hohenberg and W. Khon, *Phys. Rev.* **136**, B864 (1964).

<sup>7</sup>S. H. Vosko, L. Wilk, and N. Nusair, *Can. J. Phys.* **58**, 1200 (1980).

<sup>8</sup>A. D. Becke, *J. Chem. Phys.* **98**, 5648 (1998).

<sup>9</sup>C. Lee, W. Yang, and R. G. Parr, *Phys. Rev. B* **37**, 785 (1988).

<sup>10</sup>M. J. Frisch, G. W. Trucks, H. B. Schlegel, G. E. Scuseria, M. A. Robb, J. R. Cheeseman, V. G. Zakrzewski, J. A. Montgomery, R. E. Stratmann, J. C. Burant, S. Dapprich, J. M. Millam, A. D. Daniels, K. N. Kudin, M. C. Strain, O. Farkas, J. Tomasi, V. Barone, M. Cossi, R. Cammi, B. Mennucci, C. Pomelli, C. Adamo, S. Clifford, J. Ochterski, G. A. Petersson, P. Y. Ayala, Q. Cui, K. Morokuma, D. K. Malick, A. D. Rabuck, K. Raghavachari, J. B. Foresman, J. Cioslowski, J. V. Ortiz, B. B. Stefanov, G. Liu, A. Liashenko, P. Piskorz, I. Komaromi, R. Gomperts, R. L. Martin, D. J. Fox, T. Keith, M. A. Al-Laham, C. Y. Peng, A. Nanayakkara, C. Gonzalez, M. Challacombe, P. M. W. Gill, B. G. Johnson, W. Chen, M. W. Wong, J. L. Andres, M. Head-Gordon, E. S. Replogle, and J. A. Pople, *GAUSSIAN 98*, Gaussian Inc. Pittsburgh, PA, 1998.

<sup>11</sup>A. Ito, T. Monobe, T. Yoshii, and K. Tanaka, *Chem. Phys. Lett.*

**330**, 281 (2000).

<sup>12</sup>J. Cioslowski, *Chem. Phys. Lett.* **216**, 389 (1993).

<sup>13</sup>W. V. Steele, R. D. Chirico, N. K. Smith, W. E. Billups, P. R. Elmore, and A. E. Wheeler, *J. Phys. Chem.* **96**, 4731 (1992).

<sup>14</sup>M. Feyereisen, M. Gutowski, and J. Simons, *J. Chem. Phys.* **96**, 2926 (1992).

<sup>15</sup>C. Ze-Xian, *Chin. Phys. Lett.* **18**, 1060 (2001).

<sup>16</sup>Z. X. Wang, X. Z. Ke, Z. Y. Zhu, F. Y. Zhu, M. L. Ruan, H. Chen, R. B. Huang, and L. S. Zheng, *Phys. Lett. A* **280**, 351 (2001).

<sup>17</sup>C. Piskoti, J. Yarger, and A. Zettl, *Nature* (London) **393**, 771 (1998).

<sup>18</sup>L.-M. Peng, Z. L. Zhang, Z. Q. Xue, Q. D. Wu, Z. N. Gu, and D. G. Pettifor, *Phys. Rev. Lett.* **85**, 3249 (2000).

<sup>19</sup>M. Dewar and W. Thiel, *J. Am. Chem. Soc.* **99**, 4499 (1977).

<sup>20</sup>R. Saito, T. Takeya, T. Kimura, G. Dresselhaus, and M. S. Dresselhaus, *Phys. Rev. B* **57**, 4145 (1998).

<sup>21</sup>J. B. Foresman and Æ. Frisch, *Exploring Chemistry With Electronic Structure Methods*, 2nd Ed. (Gaussian Inc., Pittsburgh, 1996).

<sup>22</sup>Z.-H. Dong, P. Zhou, J. M. Holden, and P. C. Eklund, *Phys. Rev. B* **48**, 2862 (1993).

<sup>23</sup>F. Negri, G. Orlandi, and F. Zerbetto, *Chem. Phys. Lett.* **144**, 31 (1988).

<sup>24</sup>R. E. Stanton and M. D. Newton, *J. Phys. Chem.* **92**, 2141 (1988).

<sup>25</sup>A. D. Becke, *Phys. Rev. A* **38**, 3098 (1988).

<sup>26</sup>Y. Wang, G. T. Hager, and P. C. Eklund, *Phys. Rev. B* **45**, 14 396 (1992).

<sup>27</sup>R. Saito, G. Dresselhaus, and M. S. Dresselhaus, *Physical Properties of Carbon Nanotubes* (Imperial College Press, London, 1999), p. 38.

<sup>28</sup>X. Blasé, L. X. Benedict, E. L. Shirley, and S. G. Louie, *Phys. Rev. Lett.* **72**, 1878 (1994).